

# THE FRACTAL STRUCTURE OF ELLIPTICAL POLYNOMIAL SPIRALS

S. A. BURRELL, K. J. FALCONER, AND J. M. FRASER

**ABSTRACT.** We investigate fractal aspects of elliptical polynomial spirals, that is planar spirals with differing polynomial rates of decay in the two axis directions. We give a full dimensional analysis of these spirals, computing explicitly their intermediate, box-counting and Assouad-type dimensions. An exciting feature is that these spirals exhibit two phase transitions within the Assouad spectrum, the first natural class of fractals known to have this property. We go on to use this dimensional information to obtain bounds for the Hölder regularity of maps that can deform one spiral into another, generalising the ‘winding problem of when spirals are bi-Lipschitz equivalent to a line segment. A novel feature is the use of fractional Brownian motion and dimension profiles to bound the Hölder exponents.

*Mathematics Subject Classification 2020:* primary: 28A80

*Key words and phrases:* elliptical polynomial spiral, generalised hyperbolic spiral, box-counting dimension, Assouad dimension, Assouad spectrum, intermediate dimensions, Hölder exponents, fractional Brownian motion.

## 1. INTRODUCTION

An infinitely wound spiral is a subset of the complex plane

$$(1.1) \quad S(\phi) = \{\phi(t) \exp(it) : 1 < t < \infty\},$$

where  $\phi : [1, \infty) \rightarrow (0, \infty)$ , known as a *winding function*, is continuous, strictly decreasing and tends to zero as  $t \rightarrow \infty$ . Such forms arise throughout science and the natural world, from  $\alpha$ -models of fluid turbulence and vortex formation to the structure of galaxies [10, 18, 17, 20, 21]. The self-similarity present within these spirals makes them natural candidates for fractal analysis, and one may wish to examine the fine local structure present at the origin [3, 12]. This may be quantified via a suitable notion of fractal dimension such as box counting

---

*Date:* August 19, 2020.

(Minkowski) dimension [4, 23].

The isotropic classical definition (1.1) may be too restrictive for the modelling of general natural or abstract phenomena. Most naturally occurring spirals are anisotropic, developing in systems with inherent asymmetry, such as elliptical whirlpools forming in a flowing body of water. Another simple example arises in Newtonian mechanics: suppose a weight attached to an elastic band is rotated about an axis parallel to the ground. At high velocities the centripetal force dominates gravity and the orbit is circular. However, if the system is allowed to decelerate, the weight will follow a spiral trajectory that will become increasingly elongated in the vertical direction as the relative contribution of gravitational force grows.

To account for these scenarios, flexibility may be introduced by controlling rate of contraction in each axis and introducing an additional functional parameter. Thus, for two winding functions  $\phi, \psi : [1, \infty) \rightarrow (0, \infty)$ , we define the associated *elliptical* spiral to be

$$(1.2) \quad S(\phi, \psi) = \{\phi(t) \cos t + i\psi(t) \sin t : 1 < t < \infty\}.$$

Our results concern the family of elliptical *polynomial* spirals  $S_{p,q} = S(t^{-p}, t^{-q})$ , where  $0 < p \leq q$ , although our arguments apply more generally. If  $p = q$ , then we write  $S_{p,p} = S_p$  and (1.2) recovers the *generalised hyperbolic* spirals. Spirals such as these with polynomial winding functions typically arise in systems with an underlying dynamical process. On the other hand, spirals emerging from static settings are generally logarithmic with winding functions of the form  $\exp(-ct)$  for  $c > 0$  [12].

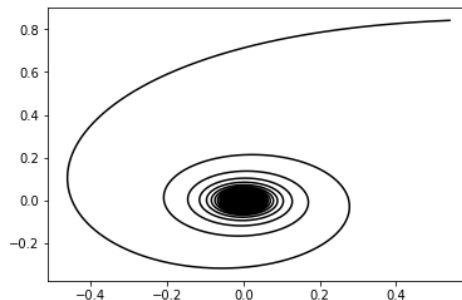


FIGURE 1. An elliptical polynomial spiral  $S_{p,q}$  with  $p = 0.7$  and  $q = 0.75$ .

This paper serves two purposes. First, we offer a dimensional analysis of the family of elliptical polynomial spirals. This involves calculating the intermediate, box-counting (Minkowski) and Assouad-type dimensions. For a thorough introduction to these dimensions we direct the reader to [4, 11]. We begin, in Theorem 2.1, by considering the intermediate dimensions of Falconer, Fraser and Kempton [7], which we denote  $\dim_\theta$  for  $\theta \in [0, 1]$  and formally define in Section 3.2. Roughly speaking, these dimensions interpolate between the Hausdorff and upper box dimensions in the sense that

$$\dim_H E \leq \dim_\theta E \leq \overline{\dim}_B E.$$

Intermediate dimensions have already seen surprising applications and properties, despite their recent introduction. For example, they have been used to establish relationships between the Hausdorff dimension of a set and the typical box dimension of fractional Brownian images [1] or orthogonal projections [2]. Other notable works include [16].

The second major notion of dimension interpolation, the Assouad spectrum of Fraser and Yu [13], lies between the upper box and Assouad dimensions and is defined in Section 3.3. One important feature of the spectrum of  $S_{p,q}$  is the presence of two points of non-differentiability, or phase transitions, see Theorem 2.6. The elliptical polynomial spirals are the first natural example to exhibit this behaviour, found before only as the product of delicate constructions.

Together, our results show the intermediate dimensions and the Assouad spectrum provide a continuous interpolation between the two extremes of the dimensional repertoire, as illustrated in Figure 2.

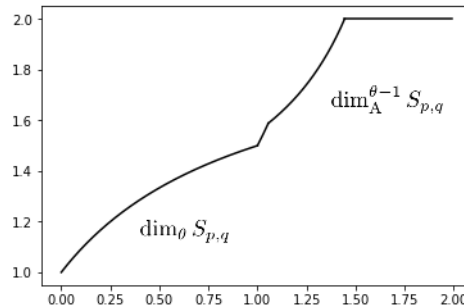


FIGURE 2. A plot of  $\dim_\theta S_{p,q}$  ( $y$ -axis) against  $\theta$  ( $x$ -axis) for  $\theta \in [0, 1]$  and  $\dim_A^{\theta-1} S_{p,q}$  against  $\theta$  for  $\theta \in [1, 2]$ . In this example,  $p = 0.1$  and  $q = 0.8$ .

The second focus is to apply the computed dimensions to determine permissible  $\alpha$  such that there may exist an  $\alpha$ -Hölder function  $f : S_{p,q} \rightarrow S_{r,s}$  that *deforms* one elliptical polynomial spiral into another. Recall a function  $f : X \rightarrow Y$  is  $\alpha$ -Hölder ( $0 < \alpha \leq 1$ ) if there exists  $c > 0$  such that

$$|f(x) - f(y)| \leq c|x - y|^\alpha \quad (x, y \in X).$$

Such maps may play a role within dynamical systems where spirals form and evolve over time. The Hölder exponent characterises the regularity of  $f$  by quantifying the degree of distortion at local scales.

A number of related questions on regularity have been explored over the past few decades for different categories of spirals that arise from winding functions of various canonical forms. Katznelson, Nag and Sullivan show that the logarithmic spiral satisfies the bi-Lipschitz *winding problem* [15]. That is, it may be constructed as the image of a bi-Lipschitz homeomorphism on the unit interval. However, if  $\phi$  decays sub-exponentially, i.e.

$$\frac{\log \phi(t)}{t} \rightarrow 0 \quad (t \rightarrow \infty),$$

then no such bi-Lipschitz homeomorphism exists [9]. This led Fraser [12] to investigate Hölder solutions to the winding problem for generalised hyperbolic spirals.

Our methodology is based on the dimension profiles of Falconer and Howroyd [8] and recent works [1, 5, 6]. Of course, if there is an  $\alpha$ -Hölder map between  $S_p$  and  $S_q$  we immediately obtain

$$(1.3) \quad \alpha \leq \frac{\dim S_p}{\dim S_q},$$

where  $\dim$  denotes Hausdorff or box dimension, since

$$\dim f(E) \leq \frac{1}{\alpha} \dim E$$

for  $E \subseteq \mathbb{R}^n$  and  $\alpha$ -Hölder  $f : \mathbb{R}^n \rightarrow \mathbb{R}^n$ . However, based on the dimension profiles, denoted  $\dim_\theta^{m\alpha} S_p$ , Theorem 2.11 provides a strictly sharper bound on  $\alpha$  by use of the formula

$$(1.4) \quad \alpha \leq \frac{\dim_\theta^{m\alpha} S_p}{\dim_\theta S_q},$$

proven by Falconer [5] in the case  $\theta = 1$  and extended to  $\theta \in [0, 1]$  by [1].

The definition of the profiles is potential-theoretic and rather challenging to compute in the case of  $S_{p,q}$ . This difficulty is circumvented by instead using their relationship [1, Theorem 3.4] to fractional Brownian images. In fact, the method employed here may be used more generally to estimate the Hölder regularity of a function between any two sets for which the box or intermediate dimensions of the fractional Brownian images may be estimated from above.

## 2. STATEMENT AND DISCUSSION OF RESULTS

This section is divided into two parts. The first offers a complete analysis of the dimensions of  $S_{p,q}$ , while the second considers applications to the Hölder regularity of maps that deform one elliptical polynomial spiral into another.

**2.1. Dimensions.** For  $0 < p \leq q$ , the Hausdorff and packing dimensions (see [4]) satisfy

$$\dim_{\text{H}} S_{p,q} = \dim_{\text{P}} S_{p,q} = 1,$$

due to the countable stability of these dimensions and the decomposition (3.1). We present the remaining dimensions of  $S_{p,q}$  in ascending order, beginning with the intermediate dimensions.

**Theorem 2.1.** *Let  $\theta \in [0, 1]$  and  $0 < p \leq q$ . If  $p < 1$ , then*

$$\dim_{\theta} S_{p,q} = \frac{p + q + 2\theta(1 - p)}{p + q + \theta(1 - p)}.$$

*Otherwise, if  $p \geq 1$ , then*

$$\dim_{\theta} S_{p,q} = 1.$$

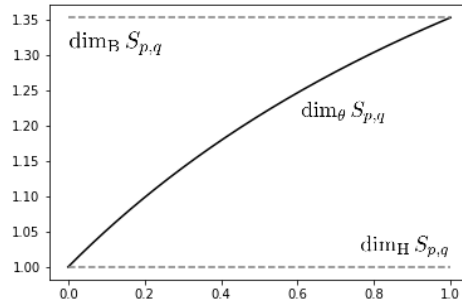


FIGURE 3. A plot of  $\dim_{\theta} S_{p,q}$  ( $y$ -axis) against  $\theta$  ( $x$ -axis) for  $p = 0.4$  and  $q = 0.7$ , along with horizontal lines that indicate  $\dim_{\text{H}} S_{p,q} = 1$  and  $\dim_{\text{P}} S_{p,q} = (2 + q - p)/(1 + q)$ .

In proving Theorem 2.1, it is convenient to prove the upper bound in the wider context of images of elliptical spirals under Hölder transformations. As we shall see, this becomes especially relevant in Section 2.2 when considering fractional Brownian images and dimension profiles.

**Lemma 2.2.** *Let  $0 < p \leq q$ ,  $\theta \in [0, 1]$  and  $f : S_{p,q} \rightarrow \mathbb{R}^2$  be  $\alpha$ -Hölder ( $0 < \alpha \leq 1$ ). If  $p < 1$ , then*

$$\overline{\dim}_\theta f(S_{p,q}) \leq \begin{cases} 2 & 0 < \alpha \leq 1/2 \\ \frac{p+q+2\theta(1-p)}{\alpha(p+q)+\theta(1-p)} & 1/2 < \alpha \leq 1 \end{cases}.$$

*Otherwise, if  $p \geq 1$ , then*

$$\overline{\dim}_\theta f(S_{p,q}) \leq \begin{cases} 2 & 0 < \alpha \leq 1/2 \\ \frac{1}{\alpha} & 1/2 < \alpha \leq 1 \end{cases}.$$

In Section 4.1, we prove Lemma 2.2 using a direct covering argument. Theorem 2.1 may then be proven by applying Lemma 2.2 to the identity map, along with a lower bound that we obtain using the mass distribution principle for intermediate dimensions [7, Proposition 2.2].

By setting  $\theta = 1$ , Theorem 2.1 also offers the box dimensions of elliptical polynomial spirals.

**Corollary 2.3.** *Let  $\theta \in [0, 1]$  and  $0 < p \leq q$ . If  $0 < p < 1$ , then*

$$\dim_B S_{p,q} = \frac{2 + q - p}{1 + q} = 1 + \frac{1 - p}{1 + q}.$$

*Otherwise, if  $p \geq 1$ , then*

$$\dim_B S_{p,q} = 1.$$

In the special case  $p = q$ , Theorem 2.1 may be applied to determine the intermediate dimensions of generalised hyperbolic spirals, which have also recently been obtained independently by Tan [19].

**Corollary 2.4.** *Let  $\theta \in [0, 1]$ . If  $0 < p < 1$ , then*

$$\dim_\theta S_p = \frac{2p + 2\theta(1 - p)}{2p + \theta(1 - p)}.$$

*Otherwise, if  $p \geq 1$ , then*

$$\dim_\theta S_p = 1.$$

A question of interest within the literature on intermediate dimensions has been the classification of sets that are continuous at  $\theta = 0$  [2, 7]. Theorem 2.1 confirms that the elliptical polynomial spirals are within this class.

**Corollary 2.5.** *Let  $0 < p \leq q$ . The function  $\theta \rightarrow \dim_\theta S_{p,q}$  is continuous on  $[0, 1]$ .*

Moving on into the realm of Assouad-type dimensions, Theorem 2.6 shows that these spirals exhibit two phase transitions, that is, points where the spectrum is non-differentiable. Moreover, these phase transitions are genuine in the sense that their left and right derivatives are necessarily distinct.

**Theorem 2.6.** *Let  $0 < p \leq q$ . If  $0 < p < 1$ , then*

$$\dim_A^\theta S_{p,q} = \begin{cases} \frac{2+q-p}{(1+q)(1-\theta)} & \text{if } 0 < \theta < p/(1+q) \\ \frac{2+q-\theta(1+q)}{(1+q)(1-\theta)} & \text{if } p/(1+q) < \theta < q/(1+q) \\ 2 & \text{if } q/(1+q) < \theta < 1 \end{cases}.$$

*Otherwise, if  $p \geq 1$ , then*

$$\dim_A^\theta S_{p,q} = \begin{cases} \frac{p-\theta(p-1)}{p(1-\theta)} & \text{if } 0 < \theta < p/(1+q) \\ \frac{2+q-\theta(1+q)}{(1+q)(1-\theta)} & \text{if } p/(1+q) < \theta < q/(1+q) \\ 2 & \text{if } q/(1+q) < \theta < 1 \end{cases}.$$

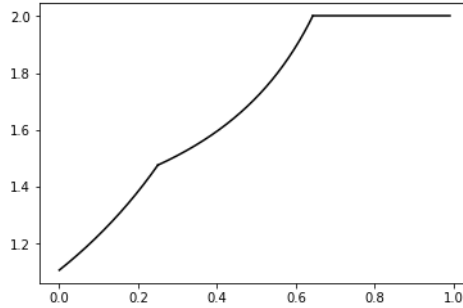


FIGURE 4. A plot of  $\dim_A^\theta S_{p,q}$  ( $y$ -axis) against  $\theta$  ( $x$ -axis) for  $p = 1.1$  and  $q = 1.8$ .

Theorem 2.6 also shows that elliptical polynomial spirals have maximal Assouad dimension.

**Corollary 2.7.** *For all  $0 < p \leq q$ ,  $\dim_A S_{p,q} = 2$ .*

The reader familiar with [12] may be surprised to see that the first phase transition occurs at  $p/(1+q)$ , rather than  $p/(1+p)$ . Indeed, this shows an unexpected and subtle interaction between the parameters.

Lastly, the relationship between elliptical polynomial spirals and concentric ellipses is worthy of consideration. Let us define

$$C_{p,q} = \bigcup_{n \in \mathbb{N}} E((2\pi n)^{-p}, (2\pi n)^{-q})$$

where  $E(x, y)$  ( $x \geq y$ ) denotes the ellipse centred on the origin with major axis of length  $2x$  and minor axis of length  $2y$ . See Figure 5. We include a short proof that  $C_{p,q}$  is dimensionally equivalent to  $S_{p,q}$ . In fact, it is not surprising our arguments apply equally well to such sets, since the covering number of  $S_{p,q}^k$  is equal to that of  $E((2\pi k)^{-p}, (2\pi k)^{-q})$  up to uniform multiplicative constants.

**Corollary 2.8.** *Theorem 2.1 and Theorem 2.6 hold with  $S_{p,q}$  replaced by  $C_{p,q}$ .*

*Proof.* This follows immediately upon observing that  $S_{p,q} \cap \{z \in \mathbb{C} : \operatorname{Re}(z) < 0\}$  is bi-Lipschitz equivalent to  $C_{p,q} \cap \{z \in \mathbb{C} : \operatorname{Re}(z) < 0\}$ .  $\square$

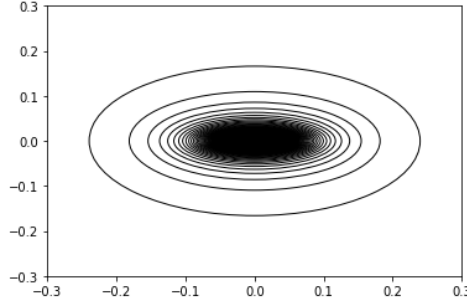


FIGURE 5. A family of concentric ellipses  $C_{p,q}$  dimensionally equivalent to  $S_{p,q}$ , where  $p = 0.4$  and  $q = 0.6$ .

**2.2. Applications.** In this section we shall see how dimension theoretic information may be applied to examine the regularity of Hölder mappings that deform one elliptical polynomial spiral into another. The behaviour of dimension under Hölder mappings has been widely studied, and offers insight into permissible  $\alpha$  for which there may exist a  $\alpha$ -Hölder map transforming a set  $X$  onto a set  $Y$ . For example, Corollary 2.3 allows us to glean such information from the box dimensions of  $S_{p,q}$  and  $S_{r,s}$ .

**Theorem 2.9.** *Let  $0 < p \leq q$  and  $0 < r \leq s$ . If  $f : S_{p,q} \rightarrow S_{r,s}$  is  $\alpha$ -Hölder, then*

$$\alpha \leq \frac{(2 + q - p)(1 + s)}{(2 + s - r)(1 + q)},$$



based on information from the box dimension. In particular, if  $p = q$  and  $r = s$ , then

$$\alpha \leq \frac{1+r}{1+p}.$$

*Proof.* By [4, Chapter 2],

$$\frac{2+s-r}{1+s} = \dim_{\text{B}} f(S_{p,q}) \leq \frac{1}{\alpha} \dim_{\text{B}} S_{p,q} = \frac{1}{\alpha} \frac{2+q-p}{1+q},$$

from which the results follow.  $\square$

Theorem 2.9 provides a non-trivial bound on  $\alpha$  when  $\dim_{\text{B}} S_{r,s} > \dim_{\text{B}} S_{p,q}$ , however, it is possible to do better using the box dimension profiles of Falconer and Howroyd [8]. Intuitively, the  $m$ -dimensional profile may be thought of as the dimension of an object when viewed from an  $m$ -dimensional viewpoint. In favour of brevity we omit a thorough introduction to dimension profiles, which may be found in [1, 2, 5, 6], since the sole property we require is their relationship to fractional Brownian images [1, 5, 22]. In the following lemma, we bound the  $2\alpha$ -profiles of  $S_{p,q}$ , denoted  $\dim_{\theta}^{2\alpha} S_{p,q}$ , by a quantity strictly less than the dimension for all  $\theta > 0$ , see Figure 6.

**Lemma 2.10.** *Let  $0 < p \leq q$  and  $\theta \in [0, 1]$ , then*

$$\dim_{\theta}^{2\alpha} S_{p,q} \leq \begin{cases} 2 & 0 < \alpha < 1/2 \\ \frac{\alpha(p+q+2\theta(1-p))}{\alpha(p+q)+\theta(1-p)} & 1/2 \leq \alpha < 1 \end{cases}.$$

*Proof.* Index- $\alpha$  fractional Brownian motion is almost-surely  $(\alpha - \varepsilon)$ -Hölder for all  $\varepsilon > 0$  [14]. Hence, for each  $\varepsilon > 0$ , Lemma 2.2 tells us that

$$\dim_{\theta} B_{\alpha}(S_{p,q}) \leq \begin{cases} 2 & 0 < \alpha \leq 1/2 \\ \frac{p+q+2\theta(1-p)}{(\alpha-\varepsilon)(p+q)+\theta(1-p)} & 1/2 < \alpha < 1 \end{cases}$$

almost-surely. Then, letting  $\varepsilon \rightarrow 0$ , by [1, Theorem 3.4] we have

$$\dim_{\theta}^{2\alpha} S_{p,q} = \alpha \dim_{\theta} B_{\alpha}(S_{p,q}) \leq \begin{cases} 2 & 0 < \alpha < 1/2 \\ \frac{\alpha(p+q+2\theta(1-p))}{\alpha(p+q)+\theta(1-p)} & 1/2 \leq \alpha < 1 \end{cases}$$

almost-surely. This concludes the proof, since  $\dim_{\theta}^{2\alpha} S_{p,q}$  has no random component.  $\square$

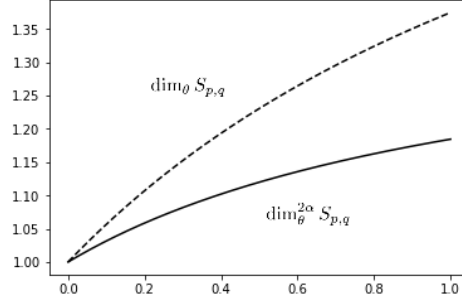


FIGURE 6. A plot of  $\dim_\theta S_{p,q}$  and the upper bound of  $\dim_\theta^{2\alpha} S_{p,q}$  ( $y$ -axis) against  $\theta$  ( $x$ -axis) for  $\alpha = 0.7$ ,  $p = 0.4$  and  $q = 0.6$ .

**Theorem 2.11.** *Let  $0 < p \leq q$  and  $0 < r \leq s$ . If  $f : S_{p,q} \rightarrow S_{r,s}$  is  $\alpha$ -Hölder, then*

$$\alpha \leq \frac{p + q + r + s - pr + qs}{(2 - r + s)(p + q)}.$$

*Proof.* It is clear that the discrepancy between the profile and the dimension is maximised when  $\theta = 1$ . Thus, set  $\theta = 1$ , and observe from Lemma 2.10 and Corollary 2.3 that

$$\dim_1 S_{r,s} = \frac{2 + s - r}{1 + s} \leq \frac{1}{\alpha} \dim_1^{2\alpha} S_{p,q} = \frac{p + q + 2(1 - p)}{\alpha(p + q) + (1 - p)},$$

from which the result follows on re-expressing the inequality in terms of  $\alpha$ .  $\square$

Recall that if  $p = q$ , then  $S_{p,p} = S_p$  is a generalised hyperbolic spiral. In this case, Theorem 2.11 offers an appealing upper bound on  $\alpha$ .

**Corollary 2.12.** *Let  $p > q$  and  $f : S_p \rightarrow S_q$  be  $\alpha$ -Hölder, then*

$$\alpha \leq \frac{p + q}{2p}.$$

*Proof.* Apply Theorem 2.11 to  $f : S_{p,p} \rightarrow S_{q,q}$ .  $\square$

It is clear from Lemma 2.10 that the bound provided by Theorem 2.11 is strictly superior to that from Theorem 2.9 for all parameter choices. This may be easily visualised in the case of  $f : S_p \rightarrow S_q$ , see Figure 7.

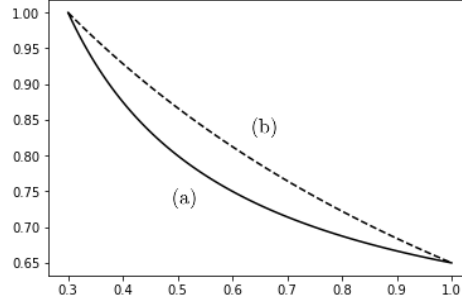


FIGURE 7. The bound on the Hölder exponent of  $f : S_p \rightarrow S_q$  ( $y$ -axis) against the value of  $p$  ( $x$ -axis) when  $q = 0.3$ . The bounds derived from the dimension profiles and the box dimension correspond to (a) and (b), respectively.

In [12], it was seen that the Assouad spectrum provided the most information on Hölder exponents in the context of the winding problem (mapping a line segment to a spiral). However, it is easily verified that the same tool, [13, Theorem 4.11], provides only trivial information in our setting (mapping a spiral to a spiral). Conversely, in the context of the winding problem, dimension profiles provide no new information. Thus, it is interesting to see that the regimes are inverted in the context of spiral deformation, with the dimension profiles providing the most information and the Assouad spectrum the least.

### 3. PRELIMINARIES

In preparation for the main proofs, we begin this subsection by setting notation and making a few technical geometric observations. Afterwards, in order to serve as a reference point, we formally define a selection of the dimension theoretic concepts. However, we assume basic familiarity with topics such as Hausdorff dimension and measure, and direct the reader to the classic text [4] for a thorough exposition on the fundamentals of dimension theory.

**3.1. Decomposition, notation, and geometric observations.** Dimension concerns limiting processes for which fixed multiplicative constants are typically of little consequence. Therefore, we often write  $x \lesssim y$  to mean there exists a universal constant  $c > 0$  not depending on  $x$  and  $y$  such that  $x \leq cy$ . Naturally, we then write  $x \gtrsim y$  if  $y \lesssim x$  and  $x \approx y$  if  $x \lesssim y$  and  $x \gtrsim y$ . In addition, we use the notation

$x \wedge y = \min\{x, y\}$  and  $x \vee y = \max\{x, y\}$ .

A useful trick is to decompose  $S_{p,q}$  into a countable disjoint union of *full turns*. In particular, we define

$$(3.1) \quad S_{p,q} := \bigcup_{k \geq 1} S_{p,q}^k,$$

where

$$S_{p,q}^k = \{t^{-p} \cos t + it^{-q} \sin t : 2\pi k \leq t < 2\pi(k+1)\}.$$

Note that, for arithmetic convenience, we have removed the part of  $S_{p,q}$  corresponding to  $1 < t < 2\pi$  in the definition (1.2) without meaningful loss of generality. The following geometric observation estimates the sum of the 1-dimensional Hausdorff measures, or length, over a collection of consecutive turns using standard number theoretic estimates.

**Lemma 3.1.** *Let  $0 < p \leq q$ . For  $k \geq 1$ ,*

$$(3.2) \quad \mathcal{H}^1(S_{p,q}^k) \approx k^{-p}.$$

*In particular, for sufficiently large integer  $N, M \in \mathbb{N}$  with  $M < N$ ,*

$$(3.3) \quad \sum_{k=M}^N \mathcal{H}^1(S_{p,q}^k) \approx \begin{cases} N^{1-p} - M^{1-p} & \text{if } p < 1 \\ \log N - \log M & \text{if } p = 1 \\ M^{1-p} - N^{1-p} & \text{if } p > 1 \end{cases}.$$

*Proof.* If  $2\pi k < t \leq 2\pi(k+1)$ , then  $t \approx k$ . (3.2) then follows from the fact  $\mathcal{H}^1(S_{p,q}^k)$  is comparable to the perimeter of an ellipse with major axis  $k^{-p}$  and minor axis  $k^{-q}$ . (3.3) may then be estimated in a standard way. If  $p \neq 1$ , we have

$$\sum_{k=M}^N \mathcal{H}^1(S_{p,q}^k) \approx \sum_{k=M}^N k^{-p} \approx \frac{1}{1-p} (N^{1-p} - M^{1-p}),$$

while the case for  $p = 1$  follows similarly.  $\square$

**3.2. Intermediate dimensions.** The intermediate dimensions are a family of dimensions, indexed by  $\theta \in [0, 1]$  and introduced in [7], that interpolate between the Hausdorff and upper box counting dimensions.

For bounded  $E \subset \mathbb{R}^n$  and  $0 < \theta \leq 1$ , the *lower intermediate dimension* of  $E$  may be defined as

$$\begin{aligned} \underline{\dim}_\theta E = \inf \{ & s \geq 0 : \text{for all } \epsilon > 0 \text{ and all } \delta_0 > 0, \text{ there exists} \\ & 0 < \delta \leq \delta_0 \text{ and a cover } \{U_i\} \text{ of } E \text{ such that} \\ & \delta \leq |U_i| \leq \delta^\theta \text{ and } \sum |U_i|^s \leq \epsilon \} \end{aligned}$$

and the corresponding *upper intermediate dimension* by

$$\begin{aligned} \overline{\dim}_\theta E = \inf \{ s \geq 0 : & \text{ for all } \epsilon > 0, \text{ there exists } \delta_0 > 0 \text{ such that} \\ & \text{ for all } 0 < \delta \leq \delta_0, \text{ there is a cover } \{U_i\} \text{ of } E \\ & \text{ such that } \delta \leq |U_i| \leq \delta^\theta \text{ and } \sum |U_i|^s \leq \epsilon \}, \end{aligned}$$

where  $|U|$  denotes the diameter of a set  $U \subset \mathbb{R}^n$ . For  $\theta = 0$ , define

$$\underline{\dim}_0 E = \overline{\dim}_0 E = \dim_H E,$$

while at  $\theta = 1$  it is clear that

$$\underline{\dim}_B E = \underline{\dim}_1 E \quad \text{and} \quad \overline{\dim}_B E = \overline{\dim}_1 E.$$

If  $\underline{\dim}_\theta E = \overline{\dim}_\theta E$  we say the  $\theta$ -intermediate dimension of  $E$  *exists* and write  $\dim_\theta E$ .

**3.3. The Assouad spectrum and dimensions.** The Assouad spectrum of  $F$ , a family of dimensions indexed by  $\theta \in [0, 1)$  and introduced in [13], interpolates between the upper box dimension and the quasi-Assouad dimension. Formally, it is the function  $\theta \mapsto \dim_A^\theta F$  defined by

$$\dim_A^\theta F = \inf \left\{ \alpha \geq 0 : \exists C > 0 \text{ such that, for all } 0 < r < 1 \text{ and } x \in F, \right. \\ \left. N_r(B(x, r^\theta) \cap F) \leq C(r^\theta/r)^\alpha \right\},$$

where  $N_r(E)$  denotes the smallest number of balls of radius  $r$  required to cover  $E$ . The Assouad dimension is defined similarly but considers  $N_r(B(x, R) \cap F)$  for arbitrary  $0 < r < R$ , thus removing the restriction on the precise relationship imposed by  $\theta$ . The limit as  $\theta \rightarrow 1$  is known as the quasi-Assouad dimension and, as we shall see, in the context of spirals is equal to the Assouad dimension. For a detailed treatment of Assouad-type dimensions and their various applications we direct the reader to [11].

## 4. PROOFS

### 4.1. Proof of Lemma 2.2.

Let  $0 \leq s \leq 2$  and  $0 < \delta < 1$ . To aid readability when dealing with particularly complicated exponents, we write  $t = -\log \delta$ .

If  $0 < \alpha \leq 1/2$ , the bound is trivial. Thus, hereafter assume  $1/2 < \alpha < 1$ .

Choose  $M \in \mathbb{N}$  to be the smallest integer satisfying

$$(4.1) \quad M \geq \exp \left( \frac{t(s - (1/\alpha) + \theta(2 - s))}{1 - p + \alpha(p + q)} \right).$$

and note that by (3.2) from Lemma 3.1,

$$N_\delta(S_{p,q}^k) \lesssim \frac{k^{-p}}{\delta}.$$

Let the uniform constant associated with the Hölder property of  $f$  be  $c > 0$ . Then, for each  $k \leq M$ , we may cover  $f(S_{p,q}^k)$  by  $ck^{-p}\delta^{-1/\alpha}$  balls of radius  $\delta$ .

The remaining region will be covered by balls of radius  $\delta^\theta$ . For  $k > M$ ,

$$\begin{aligned} \bigcup_{k > M} f(S_{p,q}^k) &\subset f([-M^{-p}, M^{-p}] \times [-M^{-q}, M^{-q}]) \\ &\subseteq [-cM^{-p\alpha}, cM^{-p\alpha}] \times [-cM^{-q\alpha}, cM^{-q\alpha}], \end{aligned}$$

and such a rectangle may be covered by

$$\approx \frac{M^{-(p+q)\alpha}}{\delta^{2\theta}}$$

balls of radius  $\delta^\theta$ . Summing over this cover, we obtain

$$(4.2) \quad \sum |U_i|^s \approx \left( \frac{M^{-\alpha(p+q)}}{\delta^{2\theta}} \right) \delta^{\theta s} + \delta^s \sum_{i=1}^M \frac{k^{-p}}{\delta^{1/\alpha}}.$$

If  $p \leq 1$ , then (4.1) and (4.2) imply

$$(4.3) \quad \begin{aligned} \sum |U_i|^s &\approx M^{-\alpha(p+q)} \delta^{\theta s - 2\theta} + M^{1-p} \delta^{s - (1/\alpha)} \\ &\approx 2 \exp \left( -t \frac{s(\alpha(p+q) + \theta(1-p)) - (p+q + 2\theta(1-p))}{1 - p + \alpha(p+q)} \right). \end{aligned}$$

Hence,  $\sum |U_i|^s \rightarrow 0$  as  $\delta \rightarrow 0$  providing

$$s > \frac{p+q + 2\theta(1-p)}{\alpha(p+q) + \theta(1-p)},$$

and so

$$\overline{\dim}_\theta f(S_{p,q}) \leq \frac{p+q + 2\theta(1-p)}{\alpha(p+q) + \theta(1-p)}.$$

On the other hand, if  $p > 1$ , then (4.2) implies

$$\begin{aligned} \sum |U_i|^s &\approx M^{-\alpha(p+q)} \delta^{\theta s - 2\theta} + \delta^{s - (1/\alpha)} \\ &\approx \exp \left( -t \frac{s(\alpha(p+q) + \theta(1-p)) - (p+q + 2\theta(1-p))}{1 - p + \alpha(p+q)} \right) + \delta^{s - (1/\alpha)}. \end{aligned}$$

Clearly,

$$1 - p + \alpha(p + q) \geq 1 - p + \frac{1}{2}(p + p) = 1,$$

and so the left-hand term converges to 0 as  $\delta \rightarrow 0$  if

$$s > \frac{p + q + 2\theta - 2p\theta}{\alpha(p + q) + \theta - p\theta},$$

while the right hand term requires  $s > 1/\alpha$ . Hence

$$\overline{\dim}_\theta f(S_{p,q}) \leq \frac{p + q + 2\theta - 2p\theta}{\alpha(p + q) + \theta - p\theta} \vee \frac{1}{\alpha} = \frac{1}{\alpha}.$$

**4.2. Proof of Theorem 2.1.** The upper bound follows from Lemma 2.2 applied to the identity mapping. If  $p \geq 1$ , the upper bound coincides with the trivial lower bound, and so it suffices to assume  $0 < p < 1$ . Let  $0 < \delta < 1$ , and define  $M$  as in (4.1). Then, set

$$s = \frac{p + q + 2\theta(1 - p)}{p + q + \theta(1 - p)},$$

and construct a measure  $\mu_\delta$  supported on  $S_{p,q}$  by

$$\mu_\delta = \delta^{s-1} \sum_{k=1}^M \mathcal{H}^1|_{S_{p,q}^k},$$

where  $\mathcal{H}^1|_{S_{p,q}^k}$  denotes the restriction of 1-dimensional Hausdorff measure to  $S_{p,q}^k$ . It is worth remarking that for a general set with a maximal  $\delta$ -sparse subset  $E$ ,

$$\delta^{s-\dim_H E} \mathcal{H}^{\dim_H E}|_E$$

may be a good candidate measure to obtain a desired target lower bound of  $s$ .

It is easy to see that

$$\mu_\delta(S_{p,q}) = \delta^{s-1} \sum_{k=1}^M \mathcal{H}^1|_{S_{p,q}^k}(S_{p,q}^k) \gtrsim \delta^{s-1} \sum_{k=1}^M k^{-p} \approx M^{1-p} \delta^{s-1} \approx 1,$$

with the final calculation identical to that which obtained (4.3).

In order to estimate  $\mu_\delta(U)$ , first note that

$$\left( \frac{1}{(k-1)^q} - \frac{1}{k^q} \right) - \left( \frac{1}{(k-1)^p} - \frac{1}{k^p} \right) = \frac{1 - (k-1)^{q-p}}{(k-1)^q} - \frac{k^{q-p} - 1}{k^q} \leq 0$$

for  $k > 1$ , since  $p \leq q$ . Hence, up to multiplicative constants, consecutive turns of the spiral are separated by at least

$$\frac{1}{(k-1)^q} - \frac{1}{k^q}.$$

An application of the mean value theorem then gives

$$\frac{1}{(k-1)^q} - \frac{1}{k^q} \geq \frac{q}{k^{q+1}} \geq \frac{q}{M^{1+q}}$$

for  $2 \leq k \leq M$ . It follows a set  $U$  satisfying  $\delta \leq |U| \leq \delta^\theta$  may intersect at most (up to a multiplicative constant)  $|U|M^{1+q}$  turns that contain mass. Moreover, for each turn it intersects,  $U$  may cover a region of mass at most  $\approx \delta^{s-1}|U|$ . Hence

$$\begin{aligned} \mu_\delta(U) &\lesssim (|U|\delta^{s-1})(|U|M^{1+q}) \\ &= |U|^2 \delta^{s-1} \delta^{-s+1-\theta(2-s)} \\ &= |U|^2 \delta^{\theta(s-2)} \\ &= |U|^2 |U|^{s-2} \text{ (since } s < 2 \text{ and } |U| \leq r^\theta) \\ &= |U|^s. \end{aligned}$$

The lower bound then follows from the mass distribution principle for intermediate dimensions, [7, Proposition 2.2].  $\square$

#### 4.3. Proof of Theorem 2.6.

If  $p = q$ , then the result is [12, Theorem 4.4], and so let  $0 < p < q$ . For each  $0 < \delta < 1$ , define  $L_p, L_q \in \mathbb{N}$  to be the largest integers such that

$$(4.4) \quad \delta \leq \frac{1}{(\pi + 2\pi L_p)^p} - \frac{1}{(\pi + 2\pi(L_p + 1))^p}$$

and

$$(4.5) \quad \delta \leq \frac{1}{(\frac{3\pi}{2} + 2\pi L_q)^q} - \frac{1}{(\frac{3\pi}{2} + 2\pi(L_q + 1))^q}.$$

Geometrically,  $L_p$  and  $L_q$  are the maximal indices  $k$ , such that  $S_{p,q}^k$  is separated on the horizontal and vertical axes by at least  $\delta$ , respectively. In addition, define the integers  $l_p$  and  $l_q$  to be the minimal  $k$  such that  $S_{p,q}^k$  intersects the ball  $B(0, \delta^\theta)$  on the horizontal and vertical axes, respectively. In particular,

$$(\pi + 2\pi l_p)^{-p} \leq \delta^\theta \leq (\pi + 2\pi(l_p - 1))^{-p}.$$

and

$$\left(\frac{3\pi}{2} + 2\pi l_q\right)^{-q} \leq \delta^\theta \leq \left(\frac{3\pi}{2} + 2\pi(l_q - 1)\right)^{-q}.$$



Throughout, we use the fact that

$$S_{p,q} \cap B(0, \delta^\theta) \subseteq \bigcup_{k=l_q}^{\infty} S_{p,q}^k \cap B(0, \delta^\theta).$$

The ordering of  $L_p, L_q, l_p$  and  $l_q$  depends on  $\theta$ , and gives rise to phase transitions within the spectrum. To determine the order based on a value of  $\theta$ , first note that  $l_t \approx \delta^{-\theta/t}$  for  $t \in \{p, q\}$ . Then, observe that for all  $t \in \{p, q\}$  an application of the mean value theorem applied to  $f(x) = x^{-t}$  gives

$$\frac{t}{(k+1)^{1+t}} \leq \frac{1}{k^t} - \frac{1}{(k+1)^t} \leq \frac{t}{k^{1+t}}.$$

This, along with the fact  $L_p$  and  $L_q$  are the minimal integers satisfying (4.4) and (4.5), respectively, implies

$$(4.6) \quad L_t \approx \delta^{-\frac{1}{1+t}}.$$

It is immediate that  $l_p > l_q$  and  $L_p > L_q$  for all  $\theta \in [0, 1)$  since  $p < q$ , but we must divide into cases to learn more. Throughout, we use the estimate

$$N_\delta(S_{p,q} \cap B(z, \delta^\theta)) \lesssim N_\delta(S_{p,q} \cap B(0, \delta^\theta))$$

for all  $z \in \mathbb{C}$ . This is intuitively clear, since the origin is the densest part of the set  $S_{p,q}$ . [13] provides further details on this reduction in the case of  $S_p$  and similar arguments would apply here.

**Case 1:**  $\frac{q}{1+q} \leq \theta < 1$ . By [13, Corollary 3.6] it suffices to consider the case  $\theta = q/(1+q)$ . For sufficiently small  $\delta$ ,

$$l_p^{-p} < L_p^{-p}$$

and

$$l_q^{-p} < L_q^{-p}.$$

Hence, for  $k \geq l_q$ , the section of  $S_{p,q}^k$  intersecting the ball  $B(0, \delta^\theta)$  is separated from neighbouring turns by less than  $\delta$  in both the horizontal and vertical directions. Thus, each grid element of a maximal  $\delta$ -grid of size approximately  $\delta^\theta$  contained within  $B(0, \delta^\theta)$  must contain a point in  $S_{p,q}^k$ . Hence

$$N_\delta(S_{p,q} \cap B(0, \delta^\theta)) \approx \left( \frac{\delta^\theta}{\delta} \right)^2$$

and the result follows.

**Case 2:**  $\frac{p}{1+q} \leq \theta \leq \frac{q}{1+q}$ . In order to simplify some geometric estimates, it is convenient to adopt an equivalent definition of the Assouad spectrum in this case. Specifically, we consider minimal coverings of the set  $D(0, \delta^\theta) \cap S_{p,q}$ , where  $D(0, \delta^\theta)$  is a square centred on the origin of side-length  $2\delta^\theta$  and orientated with the co-ordinate axes.

For sufficiently small  $\delta > 0$ ,

$$l_p^{-p} < L_q^{-p} < l_q^{-p}.$$

For  $l_q \leq k \leq L_q$ , the turn  $S_{p,q}^k \cap D(0, \delta^\theta)$  contains two disjoint arcs  $A$  and  $B$ , with one below and one above the real axis. Observe

$$\mathcal{H}^1(A) \approx \mathcal{H}^1(B) \approx \delta^\theta,$$

and so

$$N_\delta(S_{p,q}^k \cap D(0, \delta^\theta)) \approx \frac{\delta^\theta}{\delta}$$

for all  $l_q \leq k \leq L_q$ . Turns in this range of indices are at least  $\delta$ -separated in the vertical direction, and thus each must be covered individually. This gives, recalling  $L_q \approx \delta^{-1/(1+q)}$  and  $l_q \approx \delta^{-\theta/q}$ ,

$$\begin{aligned} (4.7) \quad N_\delta(S_{p,q} \cap D(0, \delta^\theta)) &\gtrsim \sum_{k=l_q}^{L_q} \delta^{\theta-1} \\ &\approx \delta^{\theta-1} \left( \delta^{-\frac{1}{1+q}} - \delta^{-\frac{\theta}{q}} \right) \\ &\gtrsim \left( \frac{\delta^\theta}{\delta} \right)^{\frac{2+q-\theta(1+q)}{(1+q)(1-\theta)}}. \end{aligned}$$

Hence

$$\dim_A^\theta S_{p,q} \geq \frac{2+q-\theta(1+q)}{(1+q)(1-\theta)}.$$

On the other hand, observe

$$\bigcup_{k=1}^{L_q} S_{p,q}^k \cap D(0, \delta^\theta) \subseteq [-\delta^\theta, \delta^\theta] \times [-L_q^{-q}, L_q^{-q}].$$

and such a rectangle may be covered by

$$\approx \frac{2\delta^\theta L_q^{-q}}{\delta^2}$$

balls of radius  $\delta$ . The remaining portion may be covered in a similar manner as in (4.7), and we conclude

$$\begin{aligned} N_\delta(S_{p,q} \cap B(0, \delta^\theta)) &\lesssim \frac{\delta^\theta L_q^{-q}}{\delta^2} + \sum_{k=l_q}^{L_q} \delta^{\theta-1} \\ &= \left(\frac{\delta^\theta}{\delta}\right)^{\frac{2+q-\theta(1+q)}{(1+q)(1-\theta)}} + \left(\frac{\delta^\theta}{\delta}\right)^{\frac{2+q-\theta(1+q)}{(1+q)(1-\theta)}} \\ &\approx \left(\frac{\delta^\theta}{\delta}\right)^{\frac{2+q-\theta(1+q)}{(1+q)(1-\theta)}}. \end{aligned}$$

**Case 3:**  $0 \leq \theta \leq \frac{p}{1+q}$ . By continuity, it suffices to assume  $\theta < \frac{p}{1+q}$ . For sufficiently small  $\delta > 0$ ,

$$L_p^{-p} < L_q^{-p} < l_p^{-p} < l_q^{-p},$$

with the gaps between the four integers  $L_p, L_q, l_p$  and  $l_q$  arbitrarily large. Then, for  $k = (2l_p), \dots, L_q$ , we have

$$S_{p,q}^k \subset B(0, \delta^\theta),$$

while the turns in this region are separated by at least  $\delta$  in the horizontal and vertical directions. Therefore they must be covered individually by at least

$$\frac{\mathcal{H}^1(S_{p,q}^k)}{\delta} \approx \frac{k^{-p}}{\delta}$$

balls of radius  $\delta$ . Hence

$$(4.8) \quad N_\delta(S_{p,q} \cap B(0, \delta^\theta)) \gtrsim \sum_{k=l_p}^{L_q} \frac{k^{-p}}{\delta}.$$

This sum may be estimated using Lemma 3.1. If  $p < 1$ , then

$$\begin{aligned} N_\delta(S_{p,q} \cap B(0, \delta^\theta)) &\gtrsim \frac{L_q^{1-p} - l_p^{1-p}}{\delta} \\ &\approx \delta^{\frac{p-1}{1+q}-1} \\ &= \left(\frac{\delta^\theta}{\delta}\right)^{\frac{2+q-p}{(1+q)(1-\theta)}}. \end{aligned}$$

On the other hand, if  $p = 1$ , then

$$\begin{aligned}
 N_\delta(S_{p,q} \cap B(0, \delta^\theta)) &\gtrsim \frac{\log(L_q) - \log(l_p)}{\delta} \\
 &\approx \delta^{-1} |\log(\delta)| \\
 (4.9) \qquad &\geq \left( \frac{\delta^\theta}{\delta} \right)^{\frac{1}{(1-\theta)}}.
 \end{aligned}$$

Finally, if  $p > 1$ , then

$$\begin{aligned}
 N_\delta(S_{p,q} \cap B(0, \delta^\theta)) &\gtrsim \frac{l_p^{1-p} - L_q^{1-p}}{\delta} \\
 &\approx \delta^{\frac{(p-1)\theta}{p} - 1} \\
 &= \left( \frac{\delta^\theta}{\delta} \right)^{\frac{p-\theta(p-1)}{p(1-\theta)}}.
 \end{aligned}$$

In each case we obtain the desired lower bound.

For the upper bound, we consider a cover of three parts. First, cover turns indexed by  $k \geq L_q$  by covering the rectangle

$$[-L_q^{-p}, L_p^{-p}] \times [-L_q^{-q}, L_p^{-q}]$$

by

$$\approx \frac{L_q^{-p} L_q^{-q}}{\delta^2}$$

balls of radius  $\delta$ . The remaining two portions may then be covered as in (4.7) and (4.8). Hence

$$N_\delta(S_{p,q} \cap B(0, \delta^\theta)) \lesssim \frac{L_q^{-p} L_q^{-q}}{\delta^2} + \sum_{k=l_p}^{L_q} \frac{k^{-p}}{\delta} + \sum_{k=l_q}^{l_p} \delta^{\theta-1}.$$

We now apply Lemma 3.1 in each case. If  $p < 1$ , then

$$\begin{aligned}
 N_\delta(S_{p,q} \cap B(0, \delta^\theta)) &\lesssim \delta^{\frac{p}{1+q} + \frac{q}{1+q} - 2} + \delta^{-1} (L_q^{1-p} - l_p^{1-p}) + \delta^{\theta-1} (l_p - l_q) \\
 &\lesssim \left( \frac{\delta^\theta}{\delta} \right)^{\frac{2+q-p}{(1-\theta)(1+q)}}.
 \end{aligned}$$

On the other hand, if  $p = 1$ , then

$$\begin{aligned}
 N_\delta(S_{p,q} \cap B(0, \delta^\theta)) &\lesssim \delta^{\frac{p}{1+q} + \frac{q}{1+q} - 2} + \delta^{-1} (\log L_q - \log l_p) + \delta^{\theta-1} (l_p - l_q) \\
 &\lesssim \left( \frac{\delta^\theta}{\delta} \right)^{\frac{1}{1-\theta}}.
 \end{aligned}$$

Finally, if  $p > 1$ , then

$$\begin{aligned} N_\delta(S_{p,q} \cap B(0, \delta^\theta)) &\lesssim \delta^{\frac{p}{1+q} + \frac{q}{1+q} - 2} + \delta^{-1}(l_p^{1-p} - L_q^{1-p}) + \delta^{\theta-1}(l_p - l_q) \\ &\lesssim \left(\frac{\delta^\theta}{\delta}\right)^{\frac{p-(p-1)\theta}{(1-\theta)p}}, \end{aligned}$$

which completes the proof.  $\square$

#### ACKNOWLEDGEMENT

SAB was supported by a *Carnegie Trust PhD Scholarship* (PHD060287). KJF and JMF were supported by an *EPSRC Standard Grant* (EP/R015104/1). JMF was also supported by a *Leverhulme Trust Research Project Grant* (RPG-2019-034).

#### REFERENCES

1. S.A. Burrell. Dimensions of fractional Brownian images, *preprint*, available at: <https://arxiv.org/abs/2002.03659>
2. S.A. Burrell, K.J. Falconer and J.M. Fraser. Projection theorems for intermediate dimensions, *Journal of Fractal Geometry (to appear)*, available at: <https://arxiv.org/abs/1907.07632>
3. Y. Dupain, M. Mendès France, C. Tricot. Dimensions des spirales, *Bulletin de la S. M. F.*, **111**, (1983), 193–201.
4. K.J. Falconer. *Fractal Geometry: Mathematical Foundations and Applications*, John Wiley & Sons, Hoboken, NJ, 3rd. ed., 2014.
5. K.J. Falconer. *A capacity approach to box and packing dimensions of projections and other images*, In Analysis, Probability and Mathematical Physics on Fractals, 1-19, World Scientific Publishing, Singapore, 2020.
6. K.J. Falconer. A capacity approach to box and packing dimensions of projections of sets and exceptional directions, *Journal of Fractal Geometry (to appear)*, available at: <https://arxiv.org/abs/1901.11014>
7. K.J. Falconer, J.M. Fraser, T. Kempton, Intermediate dimensions, *Math. Zeit. (to appear)*, available at: <https://arxiv.org/abs/1811.06493>
8. K.J. Falconer and J.D. Howroyd, Projection theorems for box and packing dimensions, *Math. Proc. Cambridge Philos. Soc.*, **119**, (1997), 269–286.
9. A. Fish and L. Paunescu. Unwinding spirals, *Methods App. Anal. (to appear)*, available at: <http://arxiv.org/abs/1603.03145>
10. C. Foias, D. D. Holmb, and E. S. Titi. The Navier-Stokes-alpha model of fluid turbulence, *Physica D*, (2001), 505–519.
11. J.M. Fraser, *Assouad Dimension and Fractal Geometry*, Cambridge University Press, Tracts in Mathematics Series, *in press*
12. J.M. Fraser, On Hölder solutions to the spiral winding problem, *preprint*, (2018), available at: <https://arxiv.org/abs/1905.07563>.
13. J.M. Fraser and H. Yu. New dimension spectra: finer information on scaling and homogeneity, *Adv. Math.*, **329**, (2018), 273–328.
14. J.P. Kahane, *Some Random Series of Functions*, Cambridge University Press, Cambridge (1985).

15. Y. Katznelson, S. Nag and D. Sullivan. On conformal welding homeomorphisms associated to Jordan curves, *Ann. Acad. Sci. Fenn. Math.*, **15**, (1990), 293–306.
16. I. Kolossváry. On the intermediate dimensions of Bedford-McMullen carpets, *preprint*, (2020), available at: <https://arxiv.org/abs/2006.14366>
17. B.B. Mandelbrot. *The Fractal Geometry of Nature*, Freeman, 1982.
18. H.K. Moffatt. *Spiral structures in turbulent flow*, Wavelets, fractals, and Fourier transforms, 317–324, *Inst. Math. Appl. Conf. Ser. New Ser.*, **43**, Oxford Univ. Press, New York, 1993.
19. J. Tan, On the intermediate dimensions of concentric spheres and related sets, *in preparation*, 2020.
20. J.C. Vassilicos. *Fractals in turbulence*, Wavelets, fractals, and Fourier transforms, 325–340, *Inst. Math. Appl. Conf. Ser. New Ser.*, **43**, Oxford Univ. Press, New York, 1993.
21. J.C. Vassilicos and J. C. R. Hunt. Fractal dimensions and spectra of interfaces with application to turbulence, *Proc. Roy. Soc. London Ser. A*, **435**, (1991), 505–534.
22. Y. Xiao, Packing dimension of the image of fractional Brownian motion, *Statist. Probab. Lett.*, **33**, (1997), 379–387.
23. D. Žubrinić and V. Županović. Box dimension of spiral trajectories of some vector fields in  $\mathbb{R}^3$ , *Qual. Theory Dyn. Syst.*, **6**, (2005), 251–272.

S.A. BURRELL, SCHOOL OF MATHEMATICS AND STATISTICS, UNIVERSITY OF ST ANDREWS, ST ANDREWS, KY16 9SS, UNITED KINGDOM.

*E-mail address*: sb235@st-andrews.ac.uk

K.J. FALCONER, SCHOOL OF MATHEMATICS AND STATISTICS, UNIVERSITY OF ST ANDREWS, ST ANDREWS, KY16 9SS, UNITED KINGDOM.

*E-mail address*: kjf@st-andrews.ac.uk

J.M. FRASER, SCHOOL OF MATHEMATICS AND STATISTICS, UNIVERSITY OF ST ANDREWS, ST ANDREWS, KY16 9SS, UNITED KINGDOM.

*E-mail address*: jmf32@st-andrews.ac.uk